

Structure of polygonal defects in graphitic carbon sheets

Sigeo Ihara and Satoshi Itoh

Central Research Laboratory, Hitachi Ltd., Kokubunji, Tokyo 185, Japan

Kazuto Akagi, Ryo Tamura, and Masaru Tsukada

Department of Physics, Graduate School of Science, University of Tokyo, Hongo 7-3-1, Bunkyo-ku, Tokyo 113, Japan

(Received 18 March 1996; revised manuscript received 25 July 1996)

Various polygonal defects which retain the three-bonded character of carbon are proposed as disclinations in graphitic carbon. The n -gonal defects, where n is an integer less than 5, are responsible for forming cones and are less stable than pentagonal defects in a hexagonal network which are responsible for forming spherical fullerenes such as C_{60} . On the other hand, the n -gonal defects, where n is greater than 6, correspond to negative wedge disclinations on the surface and leads to a negatively curved surface. Using molecular-dynamics simulations, it is found that the surfaces containing 10(deca)-, 11(hendeca)-, or 12(dodeca)-gonal defects are more stable than similarly shaped surfaces containing a multiple number of heptagons. It is also found that the surfaces which contain an n -gonal defect (with a large- n value) with a periodic folding of the surface are stable for some cases. The buckled surface with an 18(octadeca)-gonal defect in particular, which is rolling with surface distortions bending upward and downward three times around the defect, gives a stable structure. Our considerations indicate that complex structures not considered before could possibly exist. The relation of screw dislocations to polygonal defects, and their stability, are also studied. [S0163-1829(96)07444-9]

I. INTRODUCTION

Disclination,^{1,2} a rotational-type extended defect in crystals, has been the target of much research because it plays an important role in the deformation processes of metals, polymers, liquid crystals, and biological systems. Positive and negative wedge disclinations are created by removing some degree of a section of a material or by inserting one, are realized easily in surfaces such as membranes or protein coats in viruses. The cage structures of graphitic carbon are composed of hexagons (sixfold rings) of atoms, and are thus suitable for realizing wedge disclinations.

It is known that a nonplanar surface of graphitic carbon can be created by inserting pentagons or heptagons into a planar surface of graphite consisting solely of hexagons. A pentagon, a positive wedge disclination of rotation 60° obtained by removing a 60° sector from the hexagonal sheet of graphite, is responsible for creating a positively curved surface. Regular arrangements of pentagons in hexagons play an essential role in forming structures such as the well-known spherical forms of carbon (C_{60} , C_{70} , etc.), and caps of straight tubular forms on a nanometer scale.³⁻⁹

A heptagon is obtained by inserting a 60° sector into a honeycomb sheet of graphite as a negative wedge disclination of rotation 60° . It is stressed theoretically¹⁰⁻¹⁴ and experimentally¹⁵⁻¹⁹ that heptagons play an important role in forming a Gaussian negatively curved surface in fullerenes (Theoretically, an octagon has also been suggested as a means of generating Gaussian negatively curved surfaces): A theoretically proposed stable minimal surface of graphite consists only of heptagons (or octagons) in a hexagonal sheet.^{10,11} Proposed atomistic models for toroidal forms,^{12,13} and helically coiled forms,¹⁴ whose existences have been confirmed experimentally,¹⁶⁻¹⁹ are created by combining

heptagons and pentagons into a hexagonal network. The existence of heptagons in carbon nanotubes is supported by TEM (transmission electron microscopy) experiments.¹⁵ The angle of the junction between small and large radii of the tube is close to 120° , equal to that required for heptagonal disclinations.

We will use the description ‘‘polygonal defects’’ rather than ‘‘disclinations’’ because the picture of a polygonal patterning of the surface is more intuitive and atomistic than the picture of disclinations whose concept is applicable to a continuum whereby atomic configurations are smeared. A single polygonal defect other than pentagonal and heptagonal in graphitic networks, however, has not been pursued as a defect structure. As far as the authors are aware, the only exceptional and close work is by Harris, who over 20 years ago systematically considered various types of disclinations in membranous systems viewed as a continuum.^{2,20} He provided various types of positive and negative wedge disclinations in membranous systems: the most intriguing in the present context is a negative wedge disclination with a rotation of 2π rad.²⁰ Although his proposal was general and intriguing, there seems to be no proper materials in which his idea is realized, particularly at the atomic level. Nor are his proposed structures for wedge disclinations directly relevant to the honeycomb structure of graphitic carbon, which we study here.

The principal aim of the present paper is to study the existence of various types of polygonal defects in graphitic carbon other than pentagonal, heptagonal, and octagonal defects, while retaining the three-bonded nature of the sp^2 hybridization of carbon. Note that the polygonal defect is located at the core of the wedge disclination in a honeycomb sheet. The motivation for this study is to show general polygonal defects, other than pentagons and heptagons, may

play some role for more flexible connection between tubes, as compared with the case where the pentagonal and heptagonal defects are supposed to be the only allowable defects existing in carbon. Introducing polygonal defects relieves the restriction on the sizes which is imposed by the relation between the angle of a structure and the number of pentagons and heptagons. The second aim of our paper is to study the stable structures of a polygonal defect. The thermodynamical and elastic properties of the polygonal defect are studied by molecular-dynamics simulations. The combination of positively and negatively curved wedge disclinations would be more stable than the single one, and could be observed experimentally in a multiple form as pentagon-heptagon pairs on the spherical fullerenes. A random distribution of various polygons is a possible form of defect structure on the surface of the amorphous sp^2 carbon sheet.¹¹ The third aim of this paper is to study the screw dislocation which is considered to be a polygon with an infinite number of vertices. Possible combinations of structures created by these not yet considered polygons and the electronic states for these polygonal structures (disclinations) are studied in a forthcoming paper, because we are interested in various atomic configurations of a single defect form.

II. SIMULATION METHOD

A. Euler's theorem and construction of polygonal defects

The general expression of Euler's theorem in a three-dimensional network is $V - E + F = 2(1 - g)$, where F , V , and E are the number of faces, vertices, and edges, respectively, and g is the genus. For graphite, each carbon atom has three bonds, each edge is shared by two polygonal faces, and each vertex is shared by three polygons. Putting f_n equal to the number of polygons with n sides and n vertices, Euler's theorem can then be expressed as $\sum(n-6)f_n = -12(1-g)$. As can be seen from the way the polygons are constructed, the above relation holds for general polygonal defects.

A pentagon in a hexagonal network can be easily obtained by combining the remaining five 60° sectors obtained by removing a 60° sector from a graphitic sheet. A heptagon in a hexagonal network can be obtained by inserting a 60° sector into a graphitic sheet. Therefore, by combining n number of 60° sectors, an n -gonal defect is obtained in the center of the sheet (see Fig. 1). Here $n=6$ designates a graphitic sheet without a defect. When $n < 6$, the surface containing a defect becomes a positively curved one as for the case of a cone, while with $n > 6$, the surface becomes negatively curved. In this paper, the 60° sector which consists of 16 carbon atoms as shown in Fig. 1 is used.

B. Simulation details

It is well known that molecular dynamics is a powerful method for studying both structural and dynamical properties by a direct solution of the many-body equations of motion. Molecular-dynamics methods are employed to confirm the stability of the structures proposed here. Molecular dynamics consists of the following procedure: set the initial guess coordinates, then calculate the forces acting on each atom, then determine coordinates and velocities for all atoms, and then

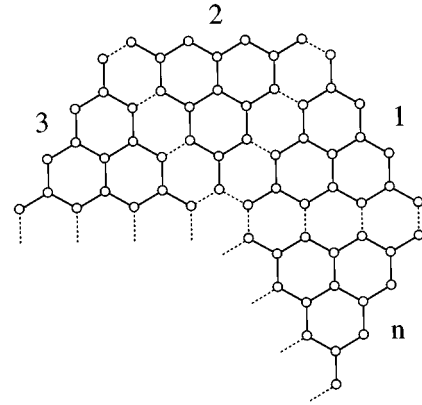


FIG. 1. Construction of the polygonal defect. An n -gonal defect is constructed by connecting n pieces of 60° sector.

repeat the procedure at each time step for the interval of interest. To calculate forces, we assume an empirical potential form for carbon atoms. Many types of empirical interatomic potentials for carbon atoms have been proposed so far. However, for the sake of simplicity, we use the Stillinger-Weber-type three-body potentials:²¹ these potential functions are shown to be descriptive of the interactions between graphitic carbon atoms.²² The following parameters optimized by Abraham and Batra for graphite²² were used: $A = 5.373\ 203\ 7$, $B = 0.508\ 245\ 71$, $a = 1.894\ 361\ 9$, $\lambda = 18.707\ 929$, and $\gamma = 1.2$. In the three-body term, the constant $\frac{1}{3}$, originally indicating the diamond structure, was replaced by $\frac{1}{2}$ to represent the honeycomb-like structure as in Ref. 23. For a calculation of the ground-state cohesive energy, the system was eventually cooled down to 0 K by using first-order equations of motion (dynamical steepest decent method). Less than 10^{-12} J/m of force acting on an atom was used as the convergence criterion. The cohesive energy per atom of the system, E , is then evaluated.

C. Evaluation of the energy of the polygonal defect

Strictly speaking, the defect energy E_d should be determined for a system with a single polygonal defect in the infinite graphitic sheet. In the simulations, however, we must cope with a finite number of atoms in a finite region. Therefore, the defect energy is estimated from the calculated energy E of the finite region system which contains N carbon atoms as

$$E_d = (EN + N_2 E_g / 3) - E_g N. \quad (1)$$

As shown in Fig. 1, the finite region we used is obtained by cutting one of the three bonds for the carbon atoms at the boundary, i.e., the boundary atom has only two bonds. The bond energy per one bond is estimated to be $E_g/3$, because each atom in the hexagonal plane has three bonds. Here E_g is the total energy per atom for the perfect hexagonal sheet obtained by molecular dynamics for a pseudoinfinite region by applying periodic boundary conditions. In the above expression, N_2 is the number of carbon atoms on the boundary. Thus the total energy of a system with a single polygonal

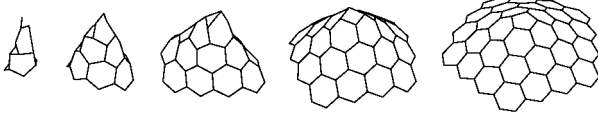


FIG. 2. Optimized conelike surfaces containing an n -gonal defect, where n is 1, 2, 3, 4, and 5.

defect in the pseudoinfinite region is obtained as $EN + N_2 E_g / 3$, and the defect energy E_d is obtained as Eq. (1).

III. RESULTS AND DISCUSSIONS

The surface containing an n -gonal defect (n -gon) is positively curved for n is less than 6, and is negatively curved surface for $n > 6$. These shapes are completely different from one another. Thus we will discuss their results separately according to whether n is greater or less than 6.

A. Positive wedge-disclination-type defects

1. Conelike surface with an ($n < 6$)-gonal defect

The conelike surface, containing a single n -gonal defect located at the center of the surface, has n -fold rotational symmetry along the axis determined by the rotational vector around the n -gonal defect when n is less than 6. Here the rotational vector is determined as a normal vector to the surface of the n -gon. Hereafter we denote a regular polygon with n vertices and n sides as an n -gon. Although n -gons for $n = 1$ and 2 are not typical geometrical figures, we treat them as polygons (n -gons) for generality. The optimized structures obtained by molecular-dynamics simulations are given in Fig. 2. From now on, n varies from left to right and top to bottom. In order to compare the structures proposed here with the TEM (transmission electron microscopy) picture obtained so far, we calculated the angle obtained by projecting the structure onto the plane surface parallel to the rotational vector of the n -gon. We refer to the angle determined here as a projection angle. Due to this definition, the projection angle changes as we change the direction of the projection while holding it perpendicular to the rotational vector. Using the symmetry of the n -gon, we adopted the average value of minimum and maximum values for the projection angles.

TABLE I. Projection angles θ and defect energies E_d of conelike structures for n -gonal defects, simple geometrical models, and multiple pentagonal defects. The deviations of the projection angles are given brackets.

n	θ ($^\circ$)			E_d (eV)	
	n -gon	model	$6-n$ pents.	n -gon	$6-n$ pents.
0			0		4.654
1	20(0)	18.3	22(15)	13.669	3.914
2	38(2)	37.1	33(23)	7.168	3.093
3	57(19)	57.0	60(2)	6.092	2.332
4	83(3)	79.1	81(24)	3.955	1.555
5	113(0)	105.5	113(0)	0.759	0.759
6	180(0)	180.0		0.0	

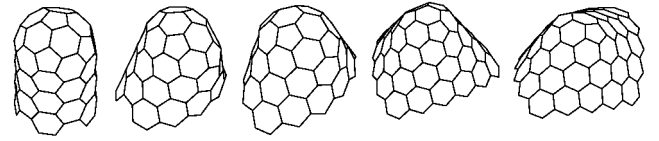


FIG. 3. Optimized conelike surfaces containing multiple pentagonal defects. The shape of the surface with $(6-n)$ pentagonal defects corresponds to the surface with an n -gonal defect ($n=0, 1, 2, 3, \text{ and } 4$).

The projection angles and their deviations are shown in Table I. For $n=3$, the deviation of the projection angle is several times larger than those of the other values of n . This is because one of the bonds forming the threefold coordination of sp^2 is broken to form more stable asymmetrical positions in contrast to the other cases where atoms of n (not equal to 3)-gons retain their symmetrical positions.

In order to show the plausibility of the values for the projection angles obtained by molecular-dynamics simulations, we compare them with angles obtained by simple geometrical considerations. Since an n -gon is in the core of a wedge disclination, the length of the arc obtained by expanding the cone containing the n -gon to the two-dimensional plane is nr ; here r is the radius of the arc or the side length of the cone. If we put the apex of the cone into the center of the sphere having radius r , the arc determined by the apex corresponds to the circle on the sphere with $nr/2\pi$ as the radius. The projection angle θ is thus evaluated from the equation $\sin(\theta/2) = n/2\pi$. As shown in Table I, good agreement between the projection angles obtained from molecular-dynamics simulations and a simple geometrical consideration is obtained.

The defect energies E_d for the surface containing an n -gon is also given in Table I. With decreasing n , the defect energy E_d increases. This indicates that the pentagon is the most stable single defect in the hexagonal network among various n -gonal defects where n is less than 6.

2. Conelike surface with multiple pentagonal defects

The shape of the structure containing a polygon with n vertices at the core of the wedge disclination can be similar to the surface containing multiple polygons with m vertices around the core of a wedge disclination if we choose a proper m which is larger than n . Note that the numbers of atoms in the different surfaces are different, although they are comparable to each other. Generally, the structure whose number of m -gons is f_m has a similar shape to the structure having a polygon with $\Sigma(6-m)f_m$ number of vertices. For instance, the conelike structure having an n -gonal defect is similar to the cone structure tiled by hexagons with $6-n$ pentagons. In Fig. 3, optimized structures for a cone having multiple pentagons are given for the corresponding single n -gon for $n = 0, 1, 2, 3, \text{ and } 4$. The pentagons are arranged so that they are not directly connected but are near each other. The projection angles of the cones are also given in Table I. If there are six pentagons, the projection angle is 0° . This pentagon case corresponds to the cap structure of carbon nanotube. The projection angles of conelike structures having multiple pentagons are almost the same as those for the corresponding single n -gonal defect. This indicates

TABLE II. Projection angles θ and defect energies E_d of saddlelike structures for n -gonal defects and multiple heptagonal defects. The deviations of the projection angles are given in parentheses.

n	θ ($^\circ$)		E_d (eV)	
	n -gon	$n-6$ hepts.	n -gon	$n-6$ hepts.
6	90(0)		0.0	0.0
7	61(1)	61(1)	0.069	0.069
8	47(0)	47(17)	0.094	0.108
9	36(1)	34(7)	0.202	0.212
10	24(6)	16(7)	0.148	0.323
11	13(3)	13(7)	0.147	0.356
12	4(1)	10(10)	0.103	0.437

that conelike structures having a certain projection angle can be considered as surfaces containing n -gonal defects, multiple pentagonal defects, and multiple types of other polygons.

The defect energies E_d for the surface containing an n -gon and corresponding to the surface with multiple pentagons are also given in Table I. With decreasing n , the defect energy E_d increases for both types of surfaces having one single n -gon, and $(6-n)$ pentagons. However, for each projection angle, the defect energy of the surface having a single n -gonal defect is higher than that the surface having $(6-n)$ pentagonal defects. Thus the surface containing $(6-n)$ pentagons is more stable than that containing a single $n(<6)$ -gonal defect. For each cone structure containing multiple pentagon, the defect energy per pentagon is almost constant and equal to 0.76–0.78 eV/atom. This indicates that distortions of the surface considered occur almost exclusively at the pentagons.

From TEM experiments, Iijima reported that the projection angle of the tip of the capped carbon nanotube observed is 19° or 40° .⁶ Later experiments^{16,23} also concluded that the sharpest capped nanotubes have about an angle of 20° . It is highly likely that 19° (20°) and 40° correspond to $n=1$ and 2 in Table II, and thus five and four pentagons, respectively, based upon our stability considerations.

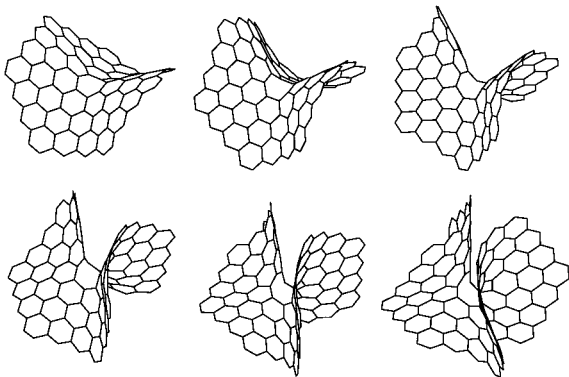


FIG. 4. Optimized saddlelike surfaces containing an n -gonal defect, where n is 7, 8, 9, 10, 11, and 12.

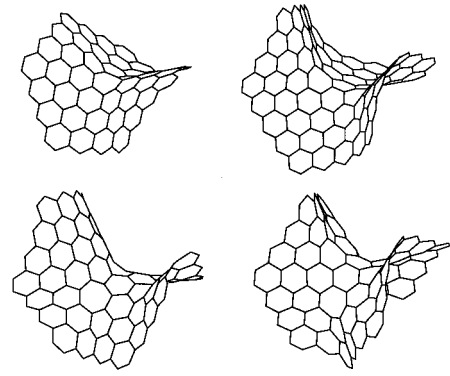


FIG. 5. Optimized saddlelike surfaces containing multiple heptagonal defects. The shape of the surface with $(n-6)$ heptagonal defects corresponds to the surface with an n -gonal defect ($n=7, 8, 9,$ and 10).

B. Negative wedge-disclination-type defects

1. Saddlelike surface with an ($n>6$)-gonal defect

The saddlelike surface containing an n -gonal defect located at the core of a wedge disclination becomes a Gaussian negatively curved surface when n is larger than 6. The optimized structures having an n -gonal defect for $n=7, 8, 9, 10, 11,$ and 12 , as predicted by molecular-dynamics simulations, are given in Fig. 4. As for the cone structures, the projection angle is determined by projecting the structure onto a plane which is parallel to the rotational vector of the n -gon. In contrast to the cone structure, the projection angle for a negatively curved surface is defined as the angle between the ridge line of the surface and the axis of the rotational vector. By this definition, the angle of the cusp appearing in the side view of the structure, as in Fig. 4, is just twice the projection angle. For saddlelike structures, we chose several ridge lines, and we used their average value to determine a projection angle. The projection angle is 90° for $n=6$ and 61° for $n=7$, and continues to decrease with increasing n . It takes on a minimum value (4°) at $n=12$. It should be noted that structure for $n=12$ corresponds to the structure of the negative wedge disclination of rotation 360° proposed by Harris over 20 years ago.²⁰ His proposal was originally made for

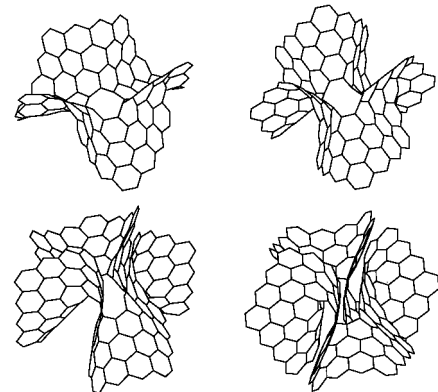


FIG. 6. Optimized buckled surfaces containing an n -gonal defect with periodicity 3, where n is 9, 12, 15, and 18.

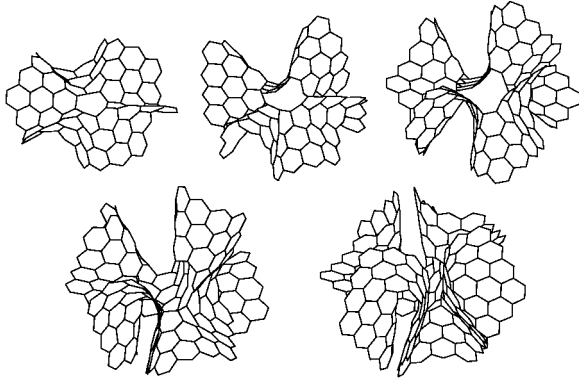


FIG. 7. Optimized buckled surfaces containing an n -gonal defect with periodicity 4, where n is 8, 12, 16, 20, and 24.

biological cell surfaces. It is interesting that corresponding structures are candidates for a defect structure in the graphite layer containing a defect of 12-gons of carbon atoms. In the graphitic surface with a 12-gonal defect as proposed here, the distance between two surfaces which face each other across the rotational axis is slightly shorter than the cutoff radius of the Stillinger-Weber potentials. However, we neglected the interaction between the two surfaces across the rotational axis, because covalent bonds should not form between graphite layers.

Defect energies for an optimized saddlelike surface with an ($n > 6$)-gonal defect are shown in Table II. The defect energies for $n=7, 8, 9, 10, 11,$ and 12 are lower than that of the surface containing a pentagonal defect (0.759 eV). Thus it is highly possible that the surface containing an n -gonal defect not only for $n=7$, but also for $n=8, 9, 10, 11,$ and 12 , may exist. It should be noted that the defect energy takes the minimum values at $n=7$, and the defect energy of $n=12$ is close to that of $n=7$. Further discussion concerning this behavior will be given later.

2. Saddlelike surface with multiple heptagonal defects

As is the case for the conelike structure, it is possible to replace an n -gon of carbon atoms with a multiplicity of polygons. Here we study the stability of saddlelike surfaces containing multiple numbers of heptagons. The heptagons are arranged so that they are not directly connected but close to one another. Some of the optimized structures for the saddlelike surfaces containing multiple heptagons is given in Fig. 5.

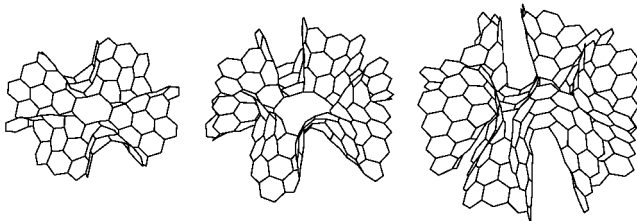


FIG. 8. Optimized buckled surfaces containing an n -gonal defect with periodicity 5, where n is 10, 15, and 20.

TABLE III. Projection angles θ of saddlelike structures for an n -gonal defect with periodicity m . The deviations of the projection angles are given in parentheses.

m	n/m				
	2	3	4	5	6
3	90(0)	57(11)	39(0)	20(12)	5.5(0)
4	68(0)	53(15)	37(0)	21(13)	6(0)
5	68(0)	51(17)	33(0)	20(7)	
6	67(0)				
7	67(0)				

The projection angles of the optimized surfaces with multiple heptagonal defects are shown in Table II. They are similar to that obtained for the saddlelike surface with a corresponding single n -gonal defect. With an increasing number of heptagons, the central position of the surface becomes ambiguous. However, for a given projection angle, we can construct a structure having ($n-6$) heptagons which is asymptotically similar to the original surface containing an n -gonal defect.

Defect energies for optimized surfaces with multiple heptagons obtained by molecular dynamics are also given in Table II. The defect energy increases roughly in proportional to the number of heptagons. For the surface containing a single polygonal defect, the defect energy increases with increasing n until $n=9$, but it decreases with increasing n after $n=9$. It should be noted that the surface with an n -gon for $n > 9$ has a lower defect energy and becomes more stable than that of the corresponding surface with $n-6$ heptagons. Thus it is possible that the surface with a 10(decagon), 11(hendecagon), or 12-gon(dodecagon) exists.

3. Buckled surface with an ($n > 6$)-gonal defect

So far, we studied saddlelike surfaces containing ($n > 6$)-gons where the surface rolls up and down twice (see Fig. 4) as we go along the edges of the n -gon. However, it is possible to create surfaces which roll more than twice as we go around the center. Here those surfaces are called buckled surfaces, and the rolling m times around the center in one cycle is denoted as the m periodicity.

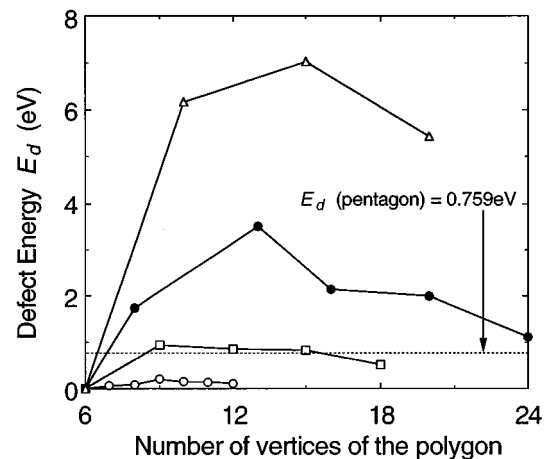


FIG. 9. Defect energies of the buckled surface containing an n -gonal defect, where n is larger than 6.

In Figs. 6, 7, and 8, the optimized surface with an n -gonal defect with $m=3, 4$, and 5, respectively, are given. We chose that the number of vertices of the polygonal defect be divisible by the number of the periodicity as typical examples. For a given number of m periodicity, we can create a surface containing a polygon with up to $n=6m$ vertices. If $n>6m$, the buckled surface folds back onto itself, and we considered it not to have relevance as the atoms are affected by strong repulsive forces. For $m=2$, as we mentioned previously, the surface with a 12-gonal(dodecagonal) defect corresponds to that proposed by Harris. For $m\geq 4$, the distance between the neighboring surfaces becomes closer than the cutoff radius of the Stillinger-Weber potentials. We neglected the interaction between layers as we did for $m=2$. For $m=3$, however, the rolling surfaces are well separated, although the interlayer interactions cannot be neglected. For $m\geq 6$, the number of rolls is so frequent that the neighboring rolling sections become so close that it is difficult to create an independent surface for $n>2m$. For $m\geq 8$, even the surface with $n=2m$ is difficult to create for the above reason.

In Table III, we show projection angles of the surfaces for $m>2$. Note that the cases of $m=3$ and $n=6$ correspond to the ideal graphitic form without defects, thus the projection angle is 90° . For fixed ratio n/m , projection angles are almost the same for a given periodicity m because the number of carbon atoms in the 60° sector is constant. As the ratio n/m increases, the projection angle decreases. Furthermore, for a plane perpendicular to the rotational axis, the buckled surfaces considered here will become symmetric or antisymmetric according to the number of times ratio n/m is even or odd.

The defect energy of a buckled surface containing a polygonal defect is plotted in Fig. 9. For fixed the number of vertices n (or the polygon), the defect energy increases with an increase in the periodicity m . For a fixed periodicity, the defect energy increases with n up to a maximum, then decreases with n . This is because curvature of the surface, consisting of hexagons, becomes large around the defect with increasing n .

The structure having the periodicity $m=2$ seems to exist because the defect energy is small. The surface with higher periodicity seems to be unstable because the defect energy is large. It should be noted, however, that the surface containing the 18-gonal (octadecagonal) defect with periodicity $m=3$ has quite a low defect energy 0.505 eV (which is lower than the pentagonal defect 0.759 eV), thus it should exist.

C. Screw disclination of n -gonal defect in the infinity of n

The screw dislocation, which has a helicoidal surface of hexagons is obtained as the infinite number n in the form of an n -gonal defect. The infinity of vertices is obtained as the vertices of the polygons coil around the fiber axis, with some periodicity keeping the bond length of the vertices constant.

We attempted to construct various types of structures. The screw dislocations are created by a combination of the parts of the helically coiled cusp and nearly planar surface layers of graphite. The structure thus obtained, however, turned out to be unstable. Although this may have arisen because the interaction between layers were not taken into account in our

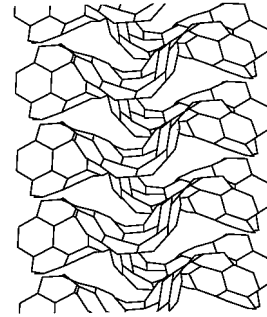


FIG. 10. Geometrical picture of the screw disclination of an n -gonal defect in the infinity of n .

simulations, a likely reason is that the stress energy around the cusp is too strong. In order to relax the stress energy to obtain a stable structure, we introduced buckling into the planar surface layers, as can be seen in Fig. 10. Stable structures for the screw dislocation we obtained are shown in Fig. 10. The cohesive energy of the screw dislocation is -6.80 eV/atom, and would exist at least as a metastable form. It is interesting to consider the combination of the screw dislocations with an antidirection of the fiber axes, because it will lead to lowering the cohesive energy by a cancellation of the stress.

IV. SUMMARY

We proposed various defect surfaces composed of hexagons and an n -gon while retaining the sp^2 bonding character of the constituent carbon atoms. Here n varies from 1 to infinity. The infinite value of n corresponds to screw dislocations in our context. It is highly possible that the defects proposed here are stable single defect forms corresponding to wedge disclinations in a graphite surface. For $n=6$, the surface becomes a hexagonal graphitic layer without defects. For $n<6$, the surface containing an n -gon becomes a cone-like surface which is less stable than the surface containing $6-n$ pentagons as defects for a corresponding projection angle. For $n>6$, the surface containing an n -gon becomes a saddlelike surface having a negative Gaussian curvature. The surface containing a 10(deca)-, 11(hendeca)-, or 12(dodeca)-gon is more stable than the surface containing four, five, or six heptagons, respectively, for a corresponding projection angle. Furthermore, the buckled surface containing an n -gon with the surface rolling up and down with more than a periodicity of 2 has the possibility of existing for a special n -gon (for instance, periodicity 3 and $n=18$).

Since the topological defect proposed here plays the important role of a scattering center for the electron transport in a hexagonal network, as pentagons and heptagons do in the hexagonal sheet and results in interesting electronic properties for the structures of graphitic surfaces such as tubes, toroidal forms, and helically coiled forms. The proposed defects and the structure obtained by combining them are candidates for further theoretical and experimental study. Combinations of proposed defects here lower the cohesive energy of the system, and can be observed experimentally in gra-

phitic form. Furthermore, the random distribution of these defects were also observed on the surface of the amorphous sp^2 carbon, as indicated by Townsend *et al.*¹¹

The electronic properties of the surface with an n -gon and screw dislocations is out of our scope of this paper, and will be discussed in a separate paper. The types of minimal sur-

face or the structure obtained by using the topological defect proposed here will be discussed in a forthcoming paper.

ACKNOWLEDGMENTS

We are grateful for the useful discussions with Dr. J. C. Greer.

-
- ¹F. R. N. Nabarro, *Dislocations* (Clarendon, London, 1967).
- ²W. F. Harris, in *Surface and Defect Properties of Solids, A Specialist Periodical Report* (Chemical Society, London, 1974), Vol. 3, p. 57.
- ³H. W. Kroto, J. R. Heath, S. C. O'Brien, R. F. Curl, and R. E. Smalley, *Nature* (London) **318**, 162 (1985); W. Krätschmer, L. D. Lamb, K. Fostiropoulos, and D. R. Huffman, *ibid.* **347**, 354 (1990). Theoretically, Osawa proposed a fullerene structure in 1970: E. Osawa, *Kagaku* (Kyoto) **25**, 854 (1970).
- ⁴F. Diederich, R. L. Whetten, C. Thilgen, R. Ettl, I. Chao, and M. M. Alvarez, *Science* **254**, 1768 (1991); K. Kikuchi, N. Nakahara, T. Wakabayashi, M. Honda, H. Matsumiya, T. Moriwaki, S. Suzuki, H. Shiromaru, K. Saito, K. Yamauchi, I. Ikemoto, and Y. Achiba, *Chem. Phys. Lett.* **188**, 177 (1992).
- ⁵D. Ugate, *Nature* (London) **359**, 707 (1992).
- ⁶S. Iijima, *Nature* (London) **354**, 56 (1991).
- ⁷T. W. Ebbesen and P. M. Ajayan, *Nature* (London) **358**, 220 (1992); J. W. Mintmire, B. I. Dunlap, and C. T. White, *Phys. Rev. Lett.* **68**, 631 (1992); N. Hamada, S. Sawada, and A. Oshiyama, *ibid.* **68**, 1579 (1992); D. H. Robertson, D. W. Brenner, and J. W. Mintmire, *Phys. Rev. B* **45**, 12 592 (1992).
- ⁸G. B. Adams, O. F. Sankey, J. B. Page, M. O'Keefe, and D. A. Drabold, *Science* **256**, 1792 (1992); H. W. Kroto, *Nature* (London) **359**, 670 (1992); D. Bakowies and W. Thiel, *J. Am. Chem. Soc.* **113**, 3704 (1991); B. L. Zang, C. H. Xu, C. Z. Wang, C. T. Chan, and K. M. Ho, *Phys. Rev. B* **46**, 7333 (1992); B. I. Dunlap, *ibid.* **47**, 4019 (1993).
- ⁹R. Saito, M. Fujita, G. Dresselhaus, and M. S. Dresselhaus, *Phys. Rev. B* **45**, 6234 (1992); R. Saito, M. Fujita, G. Dresselhaus, and M. S. Dresselhaus, *Appl. Phys. Lett.* **60**, 2204 (1992).
- ¹⁰A. L. Mackay and H. Terrones, *Nature* (London) **352**, 762 (1991); T. Lenosky, X. Gonze, M. P. Teter, and V. Elser, *ibid.* **355**, 333 (1992); D. Vanderbilt and J. Tersoff, *Phys. Rev. Lett.* **68**, 511 (1992); R. Phillips, D. A. Drabold, T. Lenosky, G. B. Adams, and O. F. Sankey, *Phys. Rev. B* **46**, 1941 (1992); W. Y. Ching, Ming-Zhu Huang, and Young-nian-Xu, *ibid.* **46**, 9910 (1992); Ming-Zhu Huang, W. Y. Ching, and T. Lenosky, *ibid.* **47**, 1593 (1992).
- ¹¹S. J. Townsend, T. J. Lenosky, D. A. Muller, C. S. Nichols, and V. Elser, *Phys. Rev. Lett.* **69**, 921 (1992).
- ¹²L. A. Chernozatonskii, *Phys. Lett. A* **170**, 37 (1992); B. I. Dunlap, *Phys. Rev. B* **46**, 1933 (1992); J. E. Avron and J. Berger, *ibid.* **51**, 1146 (1995).
- ¹³S. Itoh, S. Ihara, and J. Kitakami, *Phys. Rev. B* **47**, 1703 (1993); S. Ihara, S. Itoh, and J. Kitakami, *ibid.* **47**, 12 908 (1993); S. Itoh and S. Ihara, *ibid.* **48**, 8323 (1993).
- ¹⁴S. Ihara, S. Itoh, and J. Kitakami, *Phys. Rev. B* **48**, 5643 (1993); K. Akagi, R. Tamura, M. Tsukada, S. Itoh, and S. Ihara, *Phys. Rev. Lett.* **74**, 2307 (1995); S. Ihara and S. Itoh, *Carbon* **33**, 931 (1995).
- ¹⁵S. Iijima, P. M. Ajayan, and T. Ichihashi, *Phys. Rev. Lett.* **69**, 3100 (1992); S. Iijima, T. Ichihashi, and Y. Ando, *Nature* (London) **356**, 776 (1992).
- ¹⁶M. Endo, K. Takeuchi, K. Kobori, K. Takahashi, H. W. Kroto, and A. Sarkar, *Carbon* **33**, 873 (1995).
- ¹⁷X. F. Zhang and Z. Zhang, *Phys. Rev. B* **52**, 5313 (1995).
- ¹⁸D. Bernaerts, X. B. Zhang, X. F. Zhang, S. Amelinckx, G. Van Tendeloo, J. Van Landuyt, V. Ivanov, and J. B. Nagy, *Philos. Mag. A* **71**, 605 (1995); S. Amelinckx, X. B. Zhang, D. Bernaerts, X. F. Zhang, V. Ivanov, and J. B. Nagy, *Science* **265**, 635 (1994).
- ¹⁹C. H. Kiang, W. A. Goddard III, R. Beyers, J. R. Salem, and D. S. Bethune, *J. Phys. Chem.* **98**, 6612 (1994).
- ²⁰W. F. Harris, *Philos. Mag. A* **32**, 37 (1975); W. F. Harris and S. L. Thomas, *ibid. A* **32**, 929 (1975); W. F. Harris, *Sci. Am.* **237**, 130 (1977).
- ²¹F. H. Stillinger and T. A. Weber, *Phys. Rev. B* **31**, 5262 (1985); **33**, 1451(E) (1986). More elaborate quantum-mechanical treatments (such as a tight-binding calculation and a density-functional calculation with the pseudopotential method) or more time-consuming calculations using empirical potentials recently proposed would provide more precise results for the energies of the structures. However, our main interest lies in the feasibility or plausibility of the structure rather than a detailed comparison of the structural energies. Thus we use the Stillinger-Weber potential because of the simplicity in use in the dynamical quenching calculations.
- ²²F. F. Abraham and I. P. Batra, *Surf. Sci.* **209**, L125 (1989).
- ²³K. Sattler, *Carbon* **33**, 915 (1995).